THE JOURNAL OF BIOLOGICAL CHEMISTRY VOL. 291, NO. 36, pp. 19092–19107, September 2, 2016

Wnt-5a/Frizzled9 Receptor Signaling through the $G\alpha_o$-$G\beta\gamma$ Complex Regulates Dendritic Spine Formation*

Received for publication, February 17, 2016, and in revised form, July 2, 2016 Published, JBC Papers in Press, July 11, 2016, DOI 10.1074/jbc.M116.722132

Valerie T. Ramírez[‡], Eva Ramos-Fernández[‡], Juan Pablo Henríquez[§], Alfredo Lorenzo[¶], and Nibaldo C. Inestrosa[‡‖1]**

*From the [‡]Centro de Envejecimiento y Regeneración, Facultad de Ciencias Biológicas, Pontificia Universidad Católica de Chile, 8331150 Santiago, Chile, the [§]Laboratorio de Neurobiología del Desarrollo, Departamento de Biología Celular, Facultad de Ciencias Biológicas, Núcleo Milenio de Biología Regenerativa, Centro de Microscopía Avanzada, Universidad de Concepción, 4089100 Concepción, Chile, the [¶]Laboratorio de Neuropatología Experimental, Instituto de Investigación Médica Mercedes y Martín Ferreyra, INIMEC-CONICET, Universidad Nacional de Córdoba, 5016 Córdoba, Argentina, the [‖]Center for Healthy Brain Ageing, School of Psychiatry, Faculty of Medicine, University of New South Wales, Sydney, 2031 New South Wales, Australia, and the **Centro de Excelencia en Biomedicina de Magallanes, Universidad de Magallanes, 6200000 Punta Arenas, Chile*

Wnt ligands play crucial roles in the development and regulation of synapse structure and function. Specifically, Wnt-5a acts as a secreted growth factor that regulates dendritic spine formation in rodent hippocampal neurons, resulting in postsynaptic development that promotes the clustering of the PSD-95 (postsynaptic density protein 95). Here, we focused on the early events occurring after the interaction between Wnt-5a and its Frizzled receptor at the neuronal cell surface. Additionally, we studied the role of heterotrimeric G proteins in Wnt-5a-dependent synaptic development. We report that FZD9 (Frizzled9), a Wnt receptor related to Williams syndrome, is localized in the postsynaptic region, where it interacts with Wnt-5a. Functionally, FZD9 is required for the Wnt-5a-mediated increase in dendritic spine density. FZD9 forms a precoupled complex with $G\alpha_o$ under basal conditions that dissociates after Wnt-5a stimulation. Accordingly, we found that G protein inhibition abrogates the Wnt-5a-dependent pathway in hippocampal neurons. In particular, the activation of $G\alpha_o$ appears to be a key factor controlling the Wnt-5a-induced dendritic spine density. In addition, we found that $G\beta\gamma$ is required for the Wnt-5a-mediated increase in cytosolic calcium levels and spinogenesis. Our findings reveal that FZD9 and heterotrimeric G proteins regulate Wnt-5a signaling and dendritic spines in cultured hippocampal neurons.

The Wnt family proteins are secreted growth factors that regulate developmental processes, such as cell fate and polarity and general cell maintenance events, by modulating homeostasis and the cell cycle (1, 2). Furthermore, Wnt signaling controls various steps in the differentiation of the central nervous system (3–5), including axon guidance, dendrite development, synapse formation and plasticity (6, 7). Certain Wnt ligands, such as Wnt-7a and Wnt-3a, regulate the development and activity of the pre- and postsynaptic regions of glutamatergic synapses (8–10). Similarly, previous results have shown that Wnt-5a regulates the synaptic structure and function by inducing the clustering of PSD-95 through the activation of the c-Jun N-terminal kinase (JNK) (11) and modulates glutamate receptors through nitric oxide production (12). Additionally, Wnt-5a promotes the *de novo* formation of dendritic spines in hippocampal neurons (13) through the non-canonical Wnt/Ca^{2+} pathway.

The Frizzled (FZD)[2] family has 10 members in vertebrates and represents unconventional G protein-coupled receptors (GPCRs) (14). FZD proteins have been identified as Wnt receptors, and they can mediate the signaling triggered by several Wnt ligands. Wnt-5a activity has been linked to several FZDs receptors and other co-receptors in different model systems (15–18). However, the FZD receptor mediating Wnt-5a signaling and spine formation in hippocampal neurons has not yet been identified.

Several signaling cascades can be triggered upon Wnt binding to a FZD receptor, including canonical (*i.e.* β-catenin-dependent) and non-canonical pathways (19). Consistent with their GPCR identity, recent studies have revealed that FZD receptors can induce Wnt signaling-dependent activation of G proteins (20, 21). Heterotrimeric G proteins are composed of a guanine nucleotide-binding α-subunit (Gα) and a βγ complex (Gβγ). In the resting state, Gα is bound to GDP and associated with Gβγ and a GPCR. This complex is dissociated when Gα binds to GTP, activating Gα and the Gβγ complex, which allows them to regulate their downstream effectors (22). The Gα subunits are separated into four families based on sequence homology ($G\alpha_{i/o}$, $G\alpha_s$, $G\alpha_q$, and $G\alpha_{12/13}$) (23), each activating different pathways.

It has been shown that FZDs act as guanine nucleotide exchange factors for pertussis toxin (PTX)-sensitive G proteins *in vivo* ($G\alpha_{i/o}$), mediating both canonical and non-canonical signaling in *Drosophila* (24). In the Wnt/Ca^{2+} pathway, the G proteins, particularly the PTX-sensitive Gα

* This work was supported by FONDECYT Grant 1120156, FONDECYT Grant 1160724 and Basal Center of Excellence in Science and Technology Grant CONICYT-PFB12/2007 (to N. C. I.), a predoctoral grant (to V. T. R.), and CONICYT Postdoctoral Fellowship 3140355 (to E. R.-F.). The authors declare that they have no conflicts of interest with the contents of this article.

[1] To whom correspondence should be addressed: Centro de Envejecimiento y Regeneración, Facultad de Ciencias Biológicas, Pontificia Universidad Católica de Chile, Alameda 340, P.O. Box 114-D, Santiago, Chile. E-mail: ninestrosa@bio.puc.cl.

[2] The abbreviations used are: FZD, Frizzled; GPCR, G protein-coupled receptor; PTX, pertussis toxin; SYP, synaptophysin; AM, acetoxymethyl ester; AUC, area under the curve; DIV, day *in vitro*; CaMK, calmodulin-dependent protein kinase; PLC, phospholipase C; EGFP, enhanced green fluorescent protein; GTPγS, guanosine 5′-3-*O*-(thio)triphosphate.

subunits, have been shown to be functional in several Wnt-dependent processes (25–27). However, the role of the G proteins in Wnt-5a signaling in hippocampal neurons has not been clarified.

Here, we used hippocampal cultures, confocal fluorescent microscopy, and a combination of pharmacological and molecular approaches to characterize the cascade downstream of Wnt-5a that is relevant for dendritic spine development. Based on previous findings showing that FZD9 plays a key role in the formation of neuronal connectivity (28, 29) and that FZD9-null mice display hippocampal learning defects (30), we focused on the possible function of this receptor. We report that the activation of the non-canonical cascade by Wnt-5a required the FZD9 receptor. Also, we found that this receptor is located in the postsynaptic region, suggesting a role in Wnt-5a-induced postsynaptic remodeling. Additionally, the increase in the intracellular Ca^{2+} concentrations produced by Wnt-5a was dependent on FZD9. On the other hand, we found that FZD9 interacts with heterotrimeric G proteins, particularly the $G\alpha_o$, and that this process is crucial for the formation of dendritic spines, postsynaptic remodeling, and activation of the signaling cascade. Our results increase the comprehension of the Wnt signaling cascade in hippocampal neurons and confirm the key role of heterotrimeric G proteins in the Wnt-5a pathway.

Results

Postsynaptic Distribution of the FZD9 Receptor in Hippocampal Neurons—To determine whether FZD9 mediates the Wnt-5a spinogenic effects in hippocampal neurons, we first studied the subcellular localization of this receptor. It has been reported that FZD9 expression increases during embryonic hippocampal development (31), similar to Wnt-5a (13). However, because Wnt-5a regulates synaptic development, we first analyzed the synaptic distribution of FZD9 in cultured hippocampal neurons at day *in vitro* (DIV) 14. Our immunolocalization studies showed that FZD9 was distributed in a punctate pattern in the neuronal processes, as previously reported (31), and co-localized with the postsynaptic density scaffolding protein PSD-95 (Fig. 1*A*). This observation was supported by the Manders overlap coefficient, which represents the number of co-localized pixels expressed as a fraction of the total number of pixels in each channel. The co-localization index between PSD-95 and FZD9 was significantly higher than the co-localization between FZD9 and Piccolo, a presynaptic marker (Fig. 1*B*). Additionally, PSD-95 displays a higher co-localization index with FZD9 than those with FZD2, FZD3, or FZD7 and PSD-95, suggesting that this co-distribution was specific for FZD9 (Fig. 1*C*). The postsynaptic distribution of FZD9 was also analyzed biochemically in adult rat brains. Synaptosomal preparations were separated in the synaptophysin (SYP)-enriched (Triton X-100-soluble) fraction and the PSD-95-enriched (Triton X-100-insoluble) fraction (Fig. 1*D*). Consistent with the distribution observed in the cultured neurons, Western blotting showed that FZD9 was highly enriched in the PSD-95-containing fraction, whereas it was almost undetectable in the SYP-enriched fraction. Together, these data strongly suggest that FZD9 is located in the postsynaptic region of hippocampal neurons.

Wnt-5a Interacts with the Wnt-binding Domain of FZD9 to Increase Cytoplasmic Ca^{2+} and Dendritic Spine Density in Hippocampal Neurons—In different biological contexts, FZD9 has been shown to be a functional receptor for the ligands Wnt-2, Wnt-7a, and Wnt-8 (32–34). To assess whether FZD9 might also mediates the Wnt-5a cascade, we first performed a ligand-receptor binding assay between recombinant Wnt-5a and the cysteine-rich domain (CRD) of FZD9, which is a Wnt-binding domain (35). CRD-FZD9 (Leu^{24}–Asp^{186}) is fused to IgG. We also used the CRDs fused to IgG from FZD1, FZD2, and FZD5 to compare the interaction between Wnt-5a and these receptors. Immunoprecipitation of the CRDs-IgG chimera with A/G-agarose beads and Western blotting analysis revealed that Wnt-5a immunoprecipitated with the CRD-FZD9 as other CRD-FZDs (Fig. 2*A*). The level of immunoprecipitation of Wnt-5a was almost the same with all the CRD-FZD used, suggesting that FZD9 has a similar potential to interact biochemically with Wnt-5a. These ligand-receptor interactions are weak, because they do not interact covalently (Fig. 2*A*, *right panel*). Our biochemical assays indicates that FZD9 might be a functional receptor for Wnt-5a.

Because Wnt-5a triggers an increase in intracellular Ca^{2+} concentration in hippocampal neurons (13), we attempted to understand the potential role of FZD9 in this effect by measuring the intracellular Ca^{2+} changes using the molecular probe Fura-2 AM. As expected, Wnt-5a treatment induced a rapid increase in the intensity of the Fura-2 AM signal (340/380 ratio), indicating a positive signaling modulation in intracellular Ca^{2+}. Treatment with CRD-FZD9 blocked the Wnt-5a-mediated increase in the Ca^{2+} concentrations, whereas CRD-FZD9 has no effect (Fig. 2*B*). The area under the curve (A.U.C.) decreased from 41.20 ± 2.64 in the Wnt-5a-treated neurons to 6.81 ± 0.72 in Wnt-5a+CRD-FZD9 cells ($p < 0.001$) (Fig. 2*C*).

Previous observations have shown that Wnt-5a stimulates spinogenesis in cultured hippocampal neurons (13). Therefore, we next evaluated the potential role of CRD-FZD9 to block this process. To analyze dendritic spines, hippocampal neurons were transfected with enhanced green fluorescent protein (EGFP) at DIV 10 to reveal in detail neuronal morphology. At DIV 14 neurons were fixed and immunostained with anti-PSD-95 to label postsynaptic structures. We observed that almost all the EGFP protrusions were also labeled with anti-PSD-95, indicating that these protrusions effectively correspond to dendritic spine (Fig. 3*A*). Also, we performed a three-dimensional reconstruction of the dendrite to further analyze the dendritic spine density and the spine width head using Imaris software (Fig. 3*A*).

In agreement with previous reports (13), we observed that Wnt-5a increased the dendritic spine density (Fig. 3*B*). Interestingly, the exogenous addition of CRD-FZD9 inhibited the Wnt-5a-mediated increase in the density of dendritic protrusions after 2 h of Wnt-5a treatment.

To evaluate the potential role of the endogenous FZD9, we selectively decreased FZD9 expression using a short hairpin construct directed against FZD9 (shFZD9-EGFP) or its control

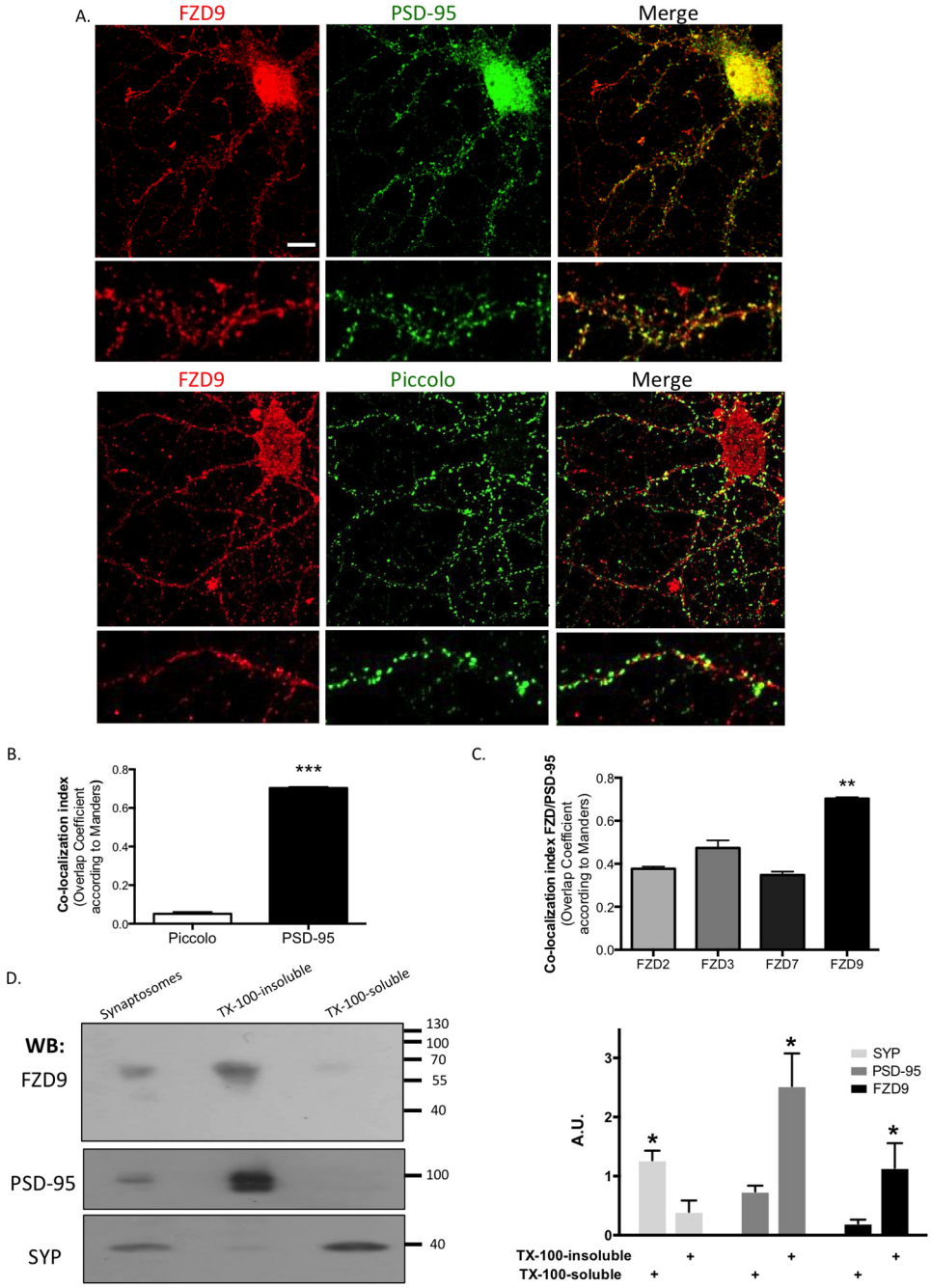

FIGURE 1. **FZD9 is located in the postsynaptic region.** *A*, representative images of DIV 14 hippocampal neuron stained with anti-PSD-95 or anti-Piccolo (*green*) and anti-FZD9 (*red*). *Scale bar*, 10 μm. *B*, quantification of the Manders co-localization index between FZD9 and PSD-95 or Piccolo ($n = 3$). *C*, quantification of the Manders co-localization index between PSD-95 and FZD2, -3, -7, and -9 ($n = 3$). *D*, detection and quantification of FZD9, PSD-95, and SYP in synaptosomes and Triton X-100-insoluble and Triton X-100-soluble-enriched membrane fractions from rat brain. The graph shows the amount of protein in each fraction normalized by the amount of the same protein in synaptosomes ($n = 5$). ***, $p < 0.001$; **, $p < 0.01$; *, $p < 0.05$. *A.U.*, arbitrary units; *WB*, Western blotting; *TX-100*, Triton X-100.

vector (Fux-EGFP). Both constructs contained the EGFP gene to label the transfected cells and have been used previously (36). FZD9 knockdown was evaluated by Western blotting in the HT22 cell line, in which a marked decrease of FZD9 expression was observed in shFZD9-EGFP-transfected cells compared with control, but it failed to decrease the FZD5 and the FZD7 expression (Fig. 4*A*). Additionally, we observed in hippocampal neurons the efficiency of the FZD9 knockdown, where the number of FZD9 clusters was reduced in shFZD9-EGFP-transfected neurons (Fig. 4*B*, *upper panel*).

Thereafter, we analyzed the effect of shFZD9-EGFP or control Fux-EGFP on Wnt-5a-induced intracellular Ca^{2+} increase in 10 DIV hippocampal neurons. In Fux-EGFP-transfected neurons, the Fura-2 AM signal increased after Wnt-5a treatment; notably, this effect was not observed in neurons transfected with shFZD9-EGFP (Fig. 4, *C* and *D*), as evidenced by the quantitative analysis. A significant reduction in A.U.C. from 1.53 ± 1.06 in the Fux-EGFP-transfected neurons to 0.44 ± 0.27 in the shFZD9-EGFP-transfected neurons ($p < 0.05$) was observed. As a control for Ca^{2+} entry, treatment with the Ca^{2+}

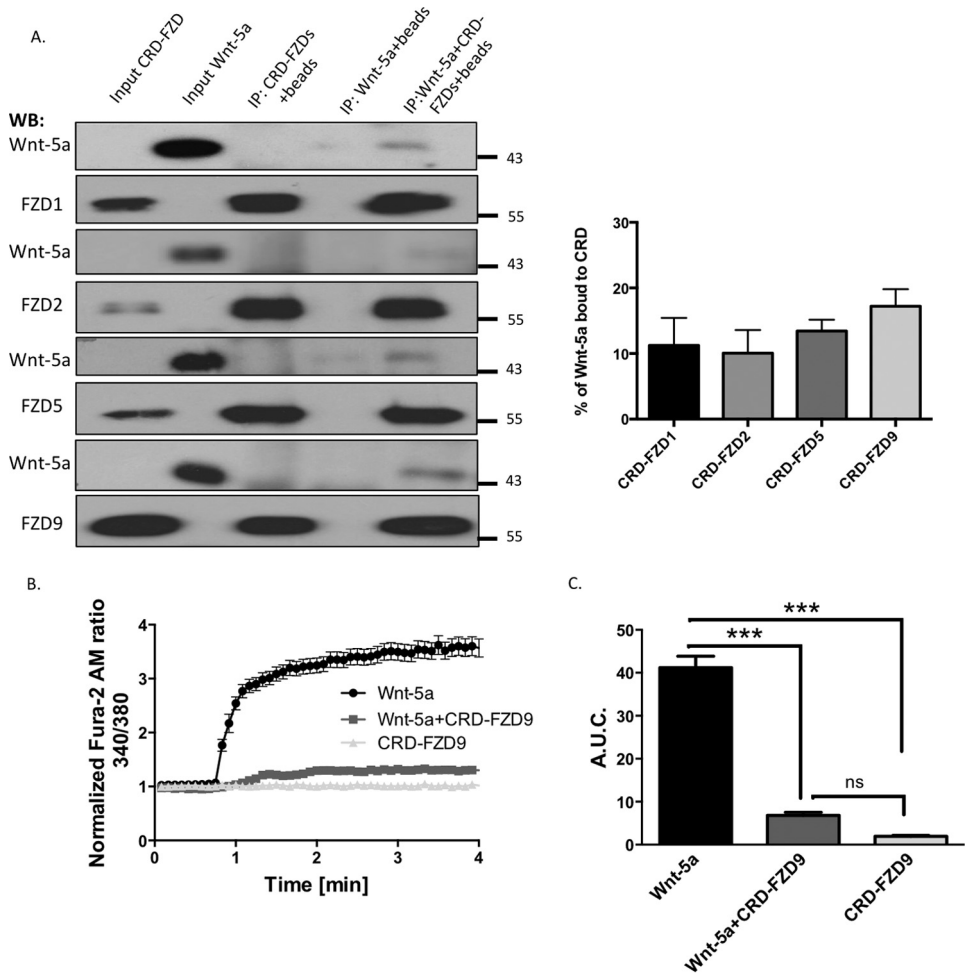

FIGURE 2. **CRD-FZD9 blocks the calcium increase produced by Wnt-5a.** *A*, recombinant Wnt-5a was incubated with protein A/G-agarose beads and CRD-FZD1, -FZD2, -FZD5, or FZD9 for 2 h. The precipitates were probed with anti-Wnt-5a and anti-FZD1, -FZD2, -FZD5, or -FZD9 antibodies. Wnt-5a (50 ng) or CRD-FZDs (50 ng) was loaded into the *left lanes* as input controls. Quantification of CRD-FZD-Wnt-5a binding assay is shown. The Wnt-5a input was considered as 100%. There was not a significant difference between the conditions ($n = 4$). *B*, measurement of intracellular Ca^{2+} in Wnt-5a, CRD-FZD9 (300 ng/ml), or Wnt-5a + CRD-FZD9-treated neurons using the Fura-2 AM probe in a 0 Ca^{2+} solution. ($n = 3$ independent experiments, 20 neurons each). *C*, quantification of the A.U.C. ($n = 3$). ***, $p < 0.001$. *WB*, Western blotting; *ns*, no significant difference; *IP*, immunoprecipitation.

ionophore ionomycin induced an intracellular Ca^{2+} increase in both neuronal populations without significant differences, suggesting that both neuronal populations can respond and produce a Ca^{2+} increase with a different stimulus than Wnt-5a (Fig. 4*C*). These experiments reveal that down-regulation of endogenous FZD9 selectively impairs the Wnt-5a-induced rapid increase in intracellular Ca^{2+} concentrations in hippocampal neurons.

Additionally, dendritic spine density was measured in shFZD9-EGFP-transfected neurons after Wnt-5a treatment. As shown in Fig. 4*E*, Wnt-5a treatment induced an increase in the number of dendritic protrusions in Fux-EGFP-transfected neurons, with a maximal effect at 2 h; however, this effect was reduced to basal levels in shFZD9-transfected neurons. To confirm these data, we used a different shRNA against FZD9 (shFZD9c-EGFP, Code number KH02416G) that is commercially available that also express the EGFP protein to select the transfected neurons, which reduce the expression of FZD9 (Fig. 4*B*, *lower panel*). In the scramble-EGFP-transfected neurons, there was a significant increase in the density of dendritic spines after the treatment with Wnt-5a (5.69 ± 1.90 spine protrusions/10-μm dendrite length) compared with control conditions (3.4 ± 1.51). This increase was not observed in shFZD9c-EGFP-transfected neurons treated with Wnt-5a (4.16 ± 1.07), as compared with the shFZD9c untreated neurons (4.30 ± 1.31) (Fig. 4*F*). Taken together, our results suggest that FZD9 mediates Wnt-5a signaling, inducing a rapid increase in the cytoplasmic Ca^{2+} concentrations and enhancing dendritic spine formation in hippocampal neurons.

Wnt-5a Specifically Activates Gα$_o$ and Decouples the FZD9-Gα$_o$-Gβ Complex in Hippocampal Neurons—To determine whether Wnt-5a activates G proteins, we performed immunoprecipitation assays using specific antibodies that recognize the GTP-bound Gα$_o$ or the Gα$_i$ subunits, the active forms of the Gα proteins (Gα$_o$-GTP or Gα$_i$-GTP), in cultures of hippocampal neurons that were previously treated with Wnt-5a for different times periods. As a positive control, the untreated lysates were incubated with the non-hydrolyzable GTP form GTPγS, which increases the activation state of G proteins. Our results show that Wnt-5a induced a sustained activation of the Gα$_o$ subunit after 5 min of exposure and

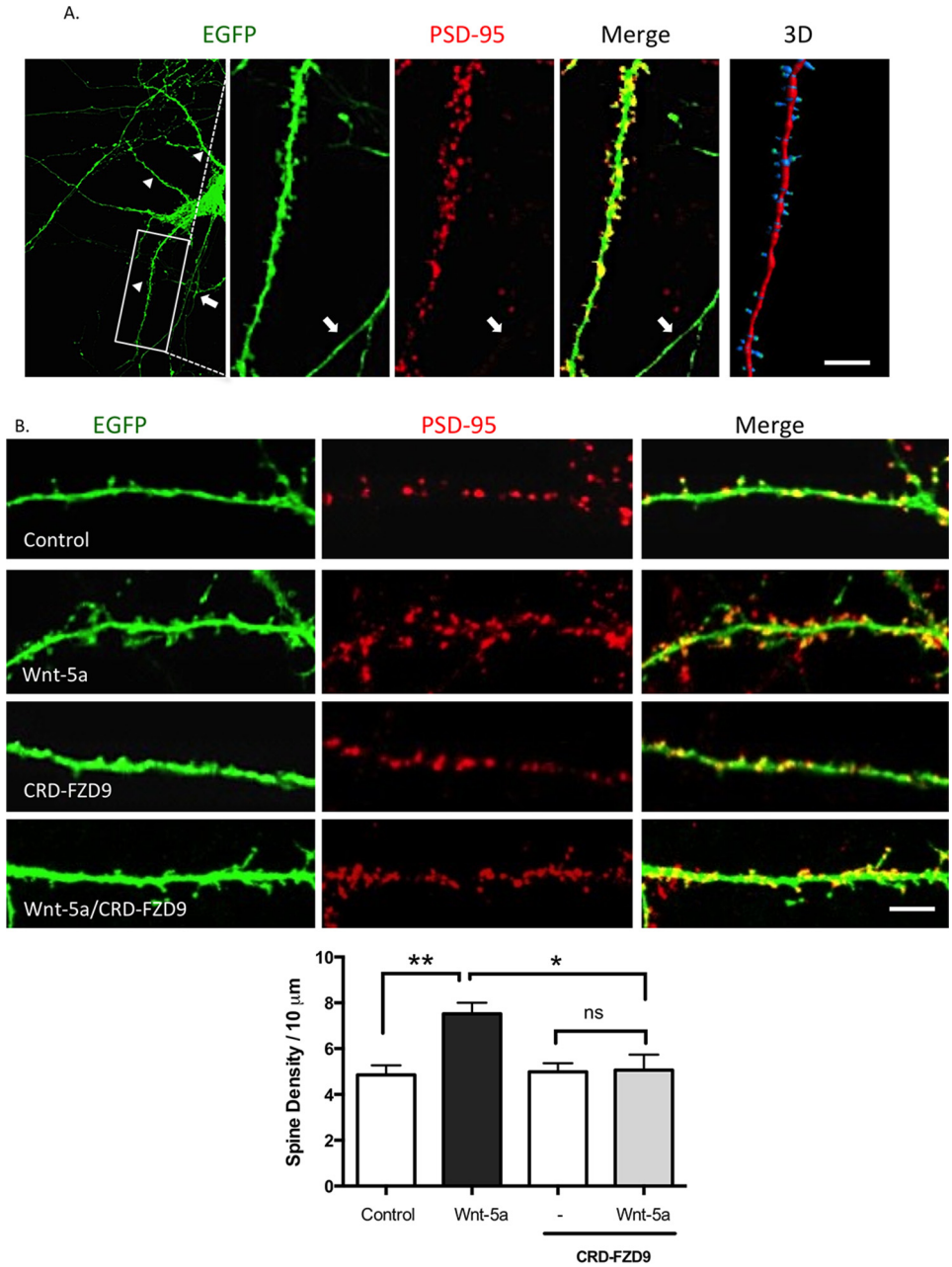

FIGURE 3. **CRD-FZD9 inhibits the spinogenesis triggered by Wnt-5a treatment.** *A*, *left*, immunodetection of PSD-95 (*red*) in EFGP-transfected neurons (*green*) maintained for 14 DIV. The *Merge* image shows the EGFP protrusion with the PSD-95 puncta stain in the head, indicating that the protrusions are spines. *Arrowheads* indicate dendrites, and *arrows* indicate an axon. *Right*, three-dimensional reconstruction of the dendrite. *Scale bar*, 25 μm. *B*, *upper panel*, representative images of EGFP-transfected neurons at DIV 10 and then treated with Wnt-5a, CRD-FZD9, or Wnt-5a+CRD-FZD9 for 2 h at DIV 14. *Lower panel*, quantification of spine density. *Scale bar*, 5 μm. ($n = 3$; 10 neurons/condition, 2–3 neurites/neuron). **, $p < 0.01$; *, $p < 0.05$.

remained active for at least 60 min. In contrast, Wnt-5a was unable to alter the level of the active $G\alpha_i$ subunit (Fig. 5*A*), suggesting that Wnt-5a specifically induces the activation of $G\alpha_o$. The IgG bands show that an equal amount of the antibody was used for each immunoprecipitation.

Considering that FZD9 mediates the Wnt-5a responses, we next aimed to determine whether FZD9 acts as a GPCR. We treated DIV 14 hippocampal neurons with Wnt-5a and then performed co-immunoprecipitation against total $G\alpha_o$. Then the precipitates were analyzed by Western blotting sequentially against $G\alpha_o$, FZD9, and $G\beta_{1-5}$ (using an antibody that labels the five Gβ isoforms) in the same membrane. We found that FZD9 receptor was markedly co-immunoprecipitated with $G\alpha_o$ in unstimulated neurons (Fig. 5*B*), suggesting that FZD9 and $G\alpha_o$ interact under basal conditions in neurons. Notably, when the neurons were treated with Wnt-5a for 30 min, the co-immunoprecipitation of FZD9 was significantly reduced. Additionally, we found that the interaction between $G\alpha_o$ and $G\beta_{1-5}$ decreases after Wnt-5a treatment, suggesting that the Gβγ complex is activated and released after the interaction between Wnt-5a and FZD9 receptor. Taken together, these results suggest that Wnt-5a decouples the interaction between and FZD9 and $G\alpha_o$ and Gβγ complex.

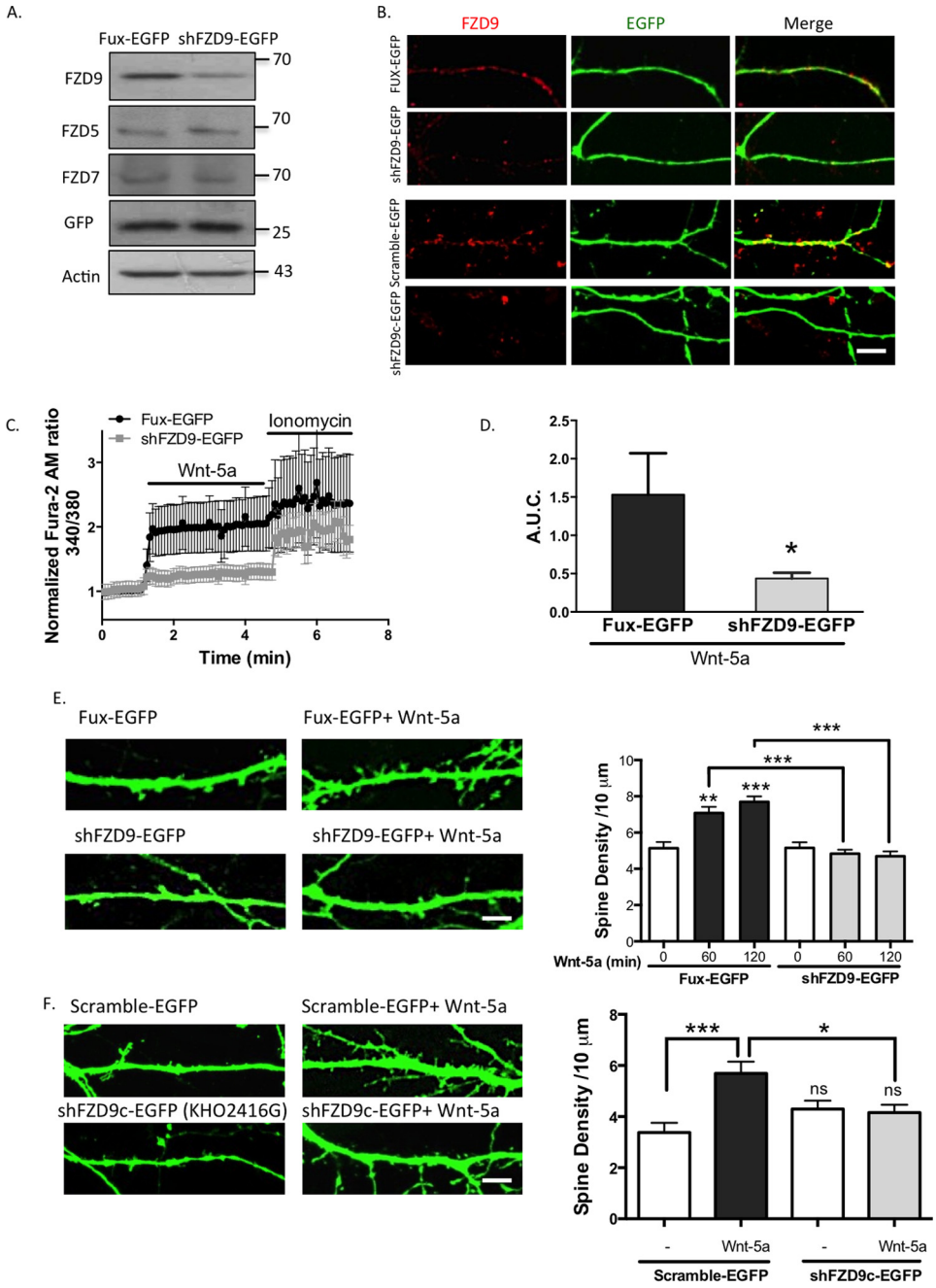

FIGURE 4. **FZD9 down-expression impairs Wnt-5a signaling.** *A*, detection of FZD9, FZD5, and FZD7 protein levels in the homogenate of HT22 cells transfected with Fux-EGFP (control) or shFZD9-EGFP (the three FZD receptors were measured in three different membranes). Anti-GFP was used as a transfection control, and anti-actin was used as a loading control ($n = 3$). *B*, immunofluorescence of FZD9 (*red*) in FUX-EGFP/shFZD9-EGFP-transfected neurons (*green*) and in scramble-EGFP/shFZD9c-EGFP (commercial shFZD9, Cod. KH02416G) transfected neurons. *Scale bar*, 8 μm. *C*, measurement of the intracellular Ca^{2+} increase in hippocampal neurons transfected with Fux-EGFP (*black plots*) or shFZD9-EGFP (*gray plots*) after stimulation with Wnt-5a. Ionomycin was used as an ionophore to increase intracellular Ca^{2+} levels. *D*, quantification of A.U.C. ($n = 4$). *E*, *left panel*, representative images of the neurites from Fux-EGFP- or shFZD9-EGFP-transfected neurons treated with or without Wnt-5a for 2 h. *Scale bar*, 3 μm. *Right panel*, quantification of the spine density in control condition or after 1 or 2 h of Wnt-5a treatment ($n = 3$). *F*, *left panel*, representative images of Scramble-EGFP and shFZD9c-EGFP-transfected neurons (commercial shFZD9, Cod. KH02416G) treated or not with Wnt-5a for 2 h. *Right panel*, quantification of the density of dendritic protrusion per neurite length. *Scale bar*, 3 μm. ***, $p < 0.001$; **, $p < 0.01$; *, $p < 0.05$. *ns*, no significant difference compared with the control.

$G\alpha_{i/o}$ Inhibition Prevents the Activation of the Non-canonical Wnt-5a Cascade in Hippocampal Neurons—Previously, it has been demonstrated that Wnt-5a activates the Wnt/Ca^{2+} and the Wnt/JNK pathways (37). In addition, Wnt-5a induces the activation of Ca^{2+}/calmodulin-dependent protein kinase IIα (CaMKIIα) and JNK in a time-dependent manner in hippocampal neurons (11, 38). To evaluate whether the effect of Wnt-5a in both cascades is due to the activation of G proteins, we analyzed the effect of PTX, an exotoxin that catalyzes the ADP-ribosylation of the $G\alpha_{i/o}$ subunits, precluding its interaction with the GPCR. First, the PTX requires an endosomal uptake, and then it is transported to the Golgi and to the endoplasmic reticulum. Finally it is released in the cytosol where it ADP-ribosylates the $G\alpha_{i/o}$ subunits (39, 40). For this reason, the hip-

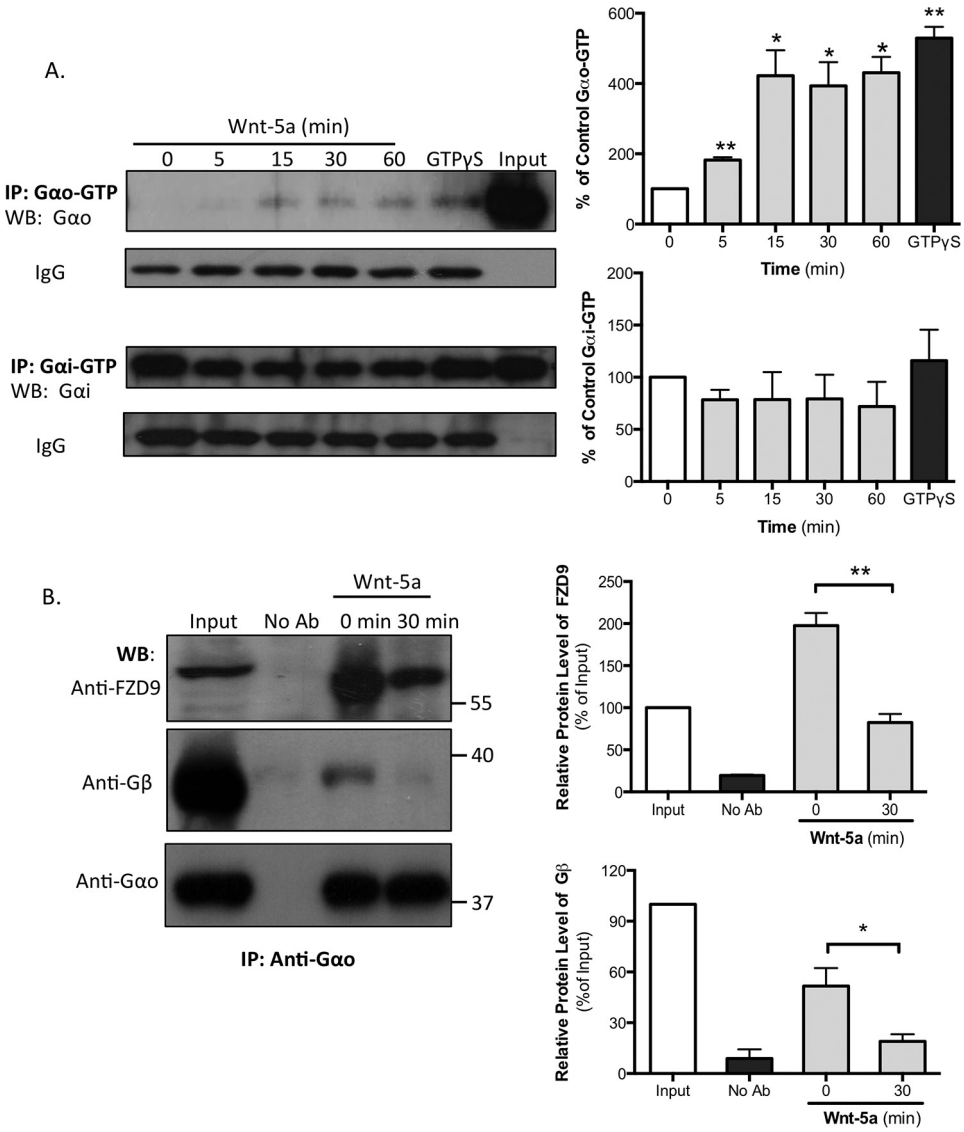

FIGURE 5. **Wnt-5a increases the GDP/GTP exchange of the Gα$_o$ subunit, and FZD9 is associated with Gα$_o$ in DIV 14 hippocampal neurons.** *A*, hippocampal neurons were stimulated with recombinant Wnt-5a for the indicated lengths of time. The lysates were incubated with specific antibodies that recognize Gα$_o$-GTP or Gα$_i$-GTP. As a positive control, untreated hippocampal neuron lysates were incubated with GTPγS for 90 min at room temperature and then incubated with the antibody. The lysates were analyzed by SDS-PAGE and immunoblotting with antibodies that recognize the total levels of Gα$_o$ or Gα$_i$ ($n = 3$). The IgG band shows that equal amounts of the Gα$_{o/i}$-GTP antibodies were used for immunoprecipitation. *Left panel*, representative blot images. *Right panel*, blot quantifications. *B*, DIV 13 or 14 neurons were treated or not with Wnt-5a (30 min), and the lysates were immunoprecipitated with an anti-Gα$_o$ antibody and immunoblotted with anti-FZD9 and anti-Gβ$_{1-5}$ (this antibody labels all five Gβ isoforms) ($n = 4$) in the same membrane. *Left panel*, representative blot images. *Right panel*, blot quantifications. **, $p < 0.01$; *, $p < 0.05$. *No Ab*, no antibody was added; *WB*, Western blotting; *IP*, immunoprecipitation.

pocampal neurons were preincubated with PTX for 6 h, and then Wnt-5a was added for different lengths of time. The hippocampal neurons showed a significant increase in the active form of CaMKIIα (p-CaMKIIα Tyr^{286}) after 30 min of Wnt-5a treatment compared with the control conditions. This effect was attenuated by preincubation with PTX at all time points (Fig. 6*A*). In addition, Wnt-5a treatment increased JNK phosphorylation (p-JNK Thr^{183}/Tyr^{185}) after 15 min, with a peak at 30 min, and this effect was also significantly reduced by PTX co-treatment (Fig. 6*A*). Additionally, we observed that exposing hippocampal neurons to Wnt-5a for 5 min induced an increase in the phosphorylation of protein kinase Cβ II (PKCβII) at serine 660, a key post-translational modification required for its translocation from the cytoplasm to the membrane and subsequent activation. Interestingly, this effect was partially blocked by PTX pretreatment (Fig. 6*A*). Finally, our findings reveal that neither Wnt-5a nor PTX affected the stabilization of β-catenin in hippocampal neurons, even after 2 h of treatment (Fig. 6*A*). These experiments confirm that Gα$_o$ is required for the activation of the non-canonical Wnt signaling pathways, including CaMKII, JNK, and PKC activation.

Because Wnt-5a promotes the clustering of PSD-95 in the postsynaptic region (11), we next analyzed the possible role of Gα$_{i/o}$ in this effect. We observed that the density of PSD-95 clustering in DIV 14 hippocampal neurons was increased at 1 and 2 h after Wnt-5a treatment compared with the controls; however, this effect was abrogated by PTX (Fig. 6*B*). In control experiments, we observed that the total PSD-95 protein levels (Fig. 6*A*) and PSD-95 clustering were unaffected after PTX treatment alone (Fig. 6*B*). Thus, our findings suggest that the

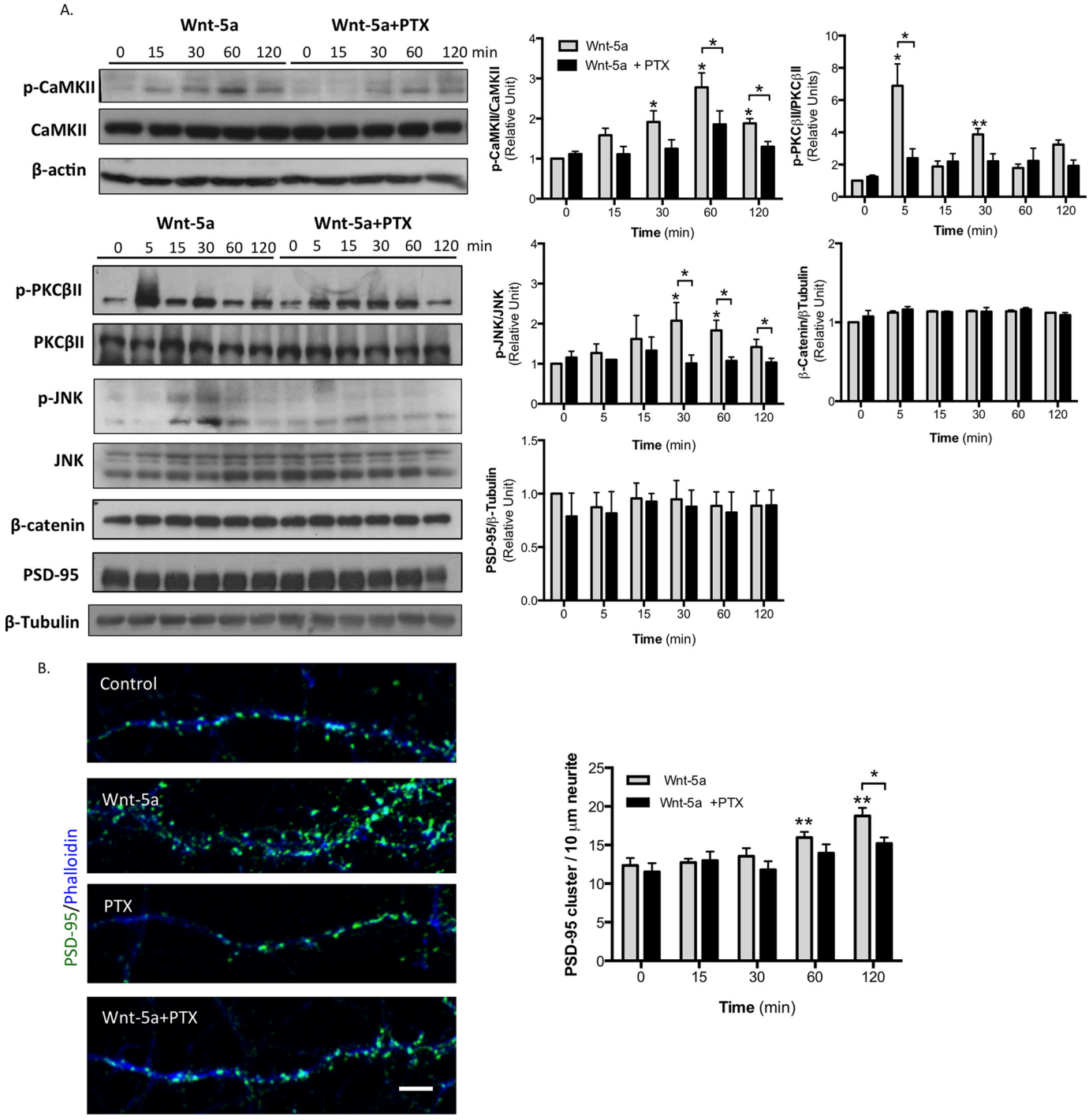

FIGURE 6. **PTX inhibits the Wnt-5a-induced activation of the non-canonical Wnt pathway in hippocampal neurons.** *A*, representative Western blotting and quantification of total and phosphorylated levels of CaMKII ($n = 4$), JNK ($n = 4$), and PKCβII ($n = 6$) and the total levels of β-catenin ($n = 3$) and PSD-95 ($n = 4$) in neurons preincubated with PTX for 6 h and then treated with Wnt-5a for the indicated lengths of time. β-Actin and β-tubulin were used as loading controls. *B*, representative images of neurites of hippocampal neurons at DIV 14 treated with recombinant Wnt-5a ligand, with PTX or with PTX plus Wnt-5a or untreated for 2 h. PSD-95 is shown in *green*, and fluorescent phalloidin-labeled actin is shown in *blue*. Quantification of the number of PSD-95 clusters/10 μm/neurite after Wnt-5a and/or PTX treatment for the indicated lengths of time ($n = 3$, 10 neurons/condition, 3 neurites/neuron) is shown. **, $p < 0.01$; *, $p < 0.05$.

activation of $G\alpha_{i/o}$ is required for Wnt-5a-induced PSD-95 clustering to promote additional postsynaptic assembly.

Wnt-5a Regulates Dendritic Spine Formation by Activating $G\alpha_o$—To identify the heterotrimeric G protein implicated in the Wnt-5a-dependent spine formation, hippocampal neurons were transfected with EGFP at DIV 10; subsequently at DIV 14 they were treated with Wnt-5a, and the effects of $G\alpha_o$, $G\alpha_i$, and $G\alpha_s$ were analyzed. The Wnt-5a-treated hippocampal neurons showed an increased dendritic spine density after 30 min of treatment, with a peak at 2 h (Fig. 7*A*). Interestingly, 6 h of pretreatment with PTX prevented the effect of Wnt-5a on dendritic spine formation. Consistent with previous results (13), the width of spine heads was increased after 120 min of Wnt-5a treatment, and this effect was inhibited after PTX treatment

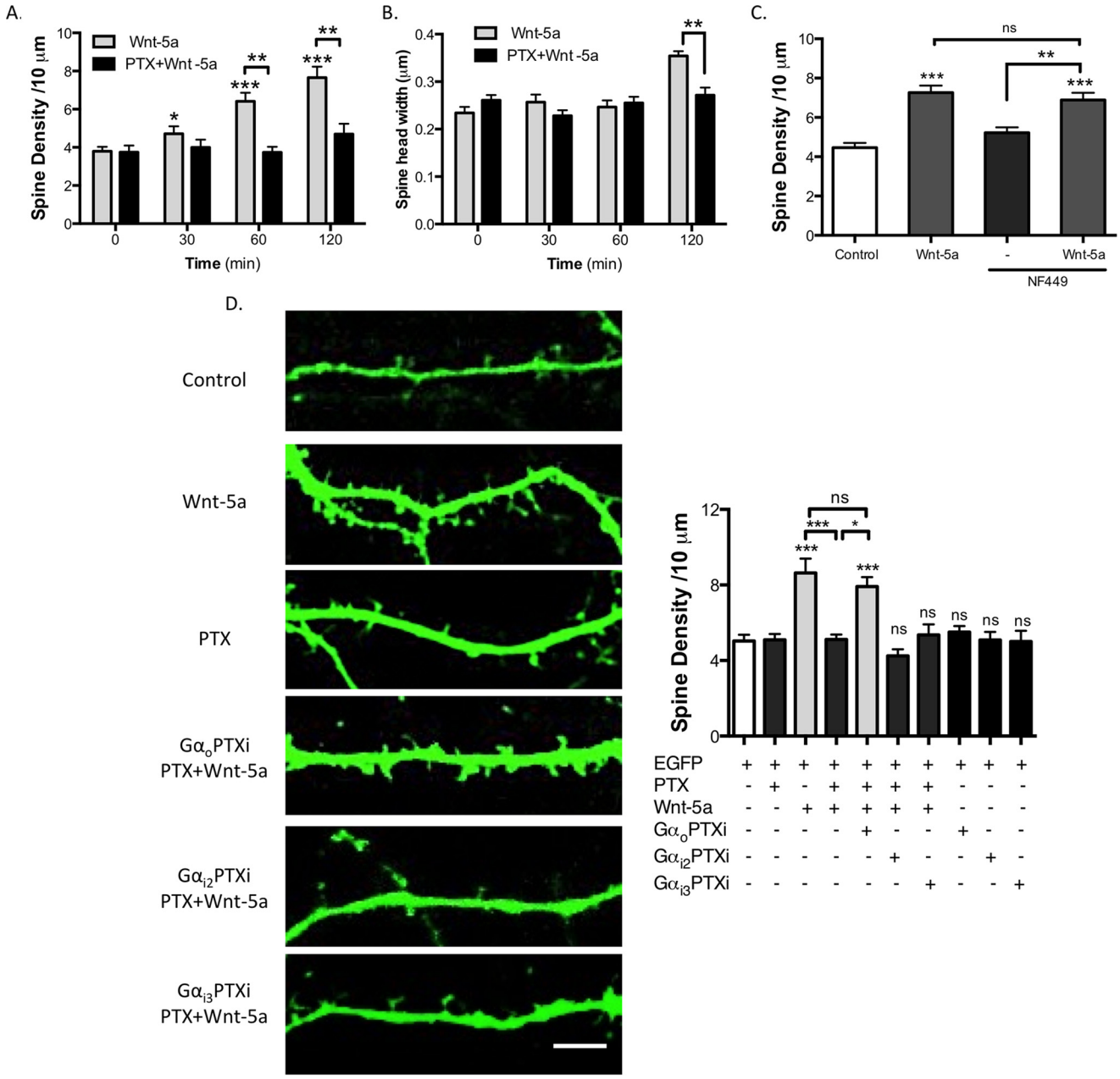

FIGURE 7. **Gα$_o$ activation is necessary for the increase in dendritic spine density stimulated by Wnt-5a.** *A*, quantification of spine density from EGFP-transfected neurons treated with or without Wnt-5a in the presence or absence of PTX. *B*, quantification of mean width of the spine heads ($n = 3$; 10 neurons/condition, 3 neurites/neuron). *C*, quantification of the spine density from EGFP-transfected neurons treated with or without Wnt-5a for 2 h in the presence or absence of NF449 (Gα$_s$ antagonist). *D*, DIV 10 hippocampal neurons were transfected with EGFP or with EGFP plus GαoPTXi, Gαi$_2$PTXi, or Gαi$_3$PTXi mutants insensitive to PTX. At DIV 14, the neurons were pretreated with PTX for 6 h and then treated with Wnt-5a for 2 h ($n = 4$). *Scale bar*, 3 μm. ***, $p < 0.001$; **, $p < 0.01$; *, $p < 0.05$. *ns*, no significant difference.

(Fig. 7*B*). The modulation of the dendritic spine density by Wnt-5a was blocked by co-treatment with sFRP2 (soluble Frizzled-related protein 2; data not shown), a Wnt scavenger that binds to Wnts and prevents their interaction with their receptors. Additionally, the Gα$_s$ subunit antagonist NF449 was used to evaluate whether this subunit is involved in the Wnt-5a signaling pathway (41). NF449 was not able to block the Wnt-5a-induced increase in the dendritic spine density, suggesting that the activation of this subunit is not required for the Wnt-5a cascade in hippocampal neurons (Fig. 7*C*). These data confirm that the spinogenic effect of Wnt-5a is mediated by activation of heterotrimeric Gα$_{i/o}$ protein.

To address whether Gα$_o$ or Gα$_i$ is implicated in the spinogenic effect of Wnt-5a, we co-transfected hippocampal neurons with EGFP and mutants forms of the Gα$_o$ (GαoPTXi) and Gα$_i$ (Gαi$_2$PTXi or Gαi$_3$PTXi) subunits that are insensitive to PTX. As shown in Fig. 7*D*, transfection with the GαoPTXi, Gαi$_2$PTXi or Gαi$_3$PTXi mutants did not affect the spine density. Importantly, the spinogenic effect of Wnt-5a that is abrogated by PTX is completely restored by transfection with the GαoPTXi, but not with the Gα$_i$PTXi subunits (Fig. 7*D*), indicating that neither the Gαi$_2$ nor the Gαi$_3$ subunits participate in the Wnt-5a-induced spine density increase. Taken together, these results suggest that Gα$_o$ activation is a key factor in the

Wnt-5a-mediated regulation of the dendritic spine morphogenesis in hippocampal neurons.

Wnt-5a Requires the Activation of the Gβγ Complex to Regulate Dendritic Spine Morphogenesis—After the activation of a GPCR, the Gβγ complex is released from the heterotrimeric G proteins to regulate multiple target proteins, including phospholipase C (PLC) and PI3K (42). It has been proposed that the Wnt/Ca^{2+} signaling pathway activates PLC through the Gβγ complex in astrocytes (43). Therefore, to address whether the activation of the Gβγ complex is involved in Wnt-5a signaling to regulate the dendritic spine density, we used Gallein, a molecule that blocks the Gβγ complex-dependent activation of PLC but does not block the interaction of Gβγ with the Gα subunits (44). Gallein was used at 5 μM, the lowest effective concentration reported in neurons (45). We measured the intracellular Ca^{2+} increase in DIV 14 hippocampal neurons treated with Wnt-5a or Wnt-5a plus Gallein. We determined that Gallein significantly diminished the increase in the Ca^{2+} concentrations after Wnt-5a treatment. Gallein decreased the A.U.C. from 5.04 ± 0.37 in Wnt-5-treated neurons to 2.71 ± 0.21 in Wnt-5a + Gallein-treated neurons ($p < 0.001$; Fig. 8*A* and *B*). Additionally, Gallein treatment blocked the Wnt-5a-mediated increase in the dendritic spine density, without disturbing the formation of the dendritic spines themselves (Fig. 8*C*). Finally, to further confirm the requirement of Gβγ complex in the spinogenic effect of Wnt-5a, hippocampal neurons were transfected with the β-adrenergic receptor kinase C-terminal peptide (βARKct), a universal competitor that sequester Gβγ and block its downstream signaling plus EGFP (46). We found that βARKct expression inhibited the Wnt-5a-mediated increase in the dendritic spine density (Fig. 8*D*). These data reveal that Gβγ activation is a key step in the Wnt-5a cascade to regulate the non-canonical Wnt signaling pathway and to modulate dendritic spine remodeling.

Discussion

The Wnt-5a ligand has been linked to cognitive and memory functions in the adult brain (7, 47). Wnt-5a regulates excitatory synaptic transmission in hippocampal neurons (48–50), including the production of nitric oxide, which triggers the expression of NMDA receptors (12) and promotes the induction of long term potentiation (51). These findings indicate that Wnt-5a is a relevant neural factor for the regulation and maintenance of the structure and function of synapses in the central nervous system. Therefore, understanding the mechanism by which Wnt-5a controls spinogenesis represents a crucial advance in the field.

Because previous studies have established that FZD9 is highly expressed in the hippocampus (31, 52), we focused our research on this Wnt receptor. Our findings show that FZD9 co-localizes with postsynaptic proteins in cultured hippocampal neurons, which is consistent with previous data showing the postsynaptic distribution of FZD9 in developing neuromuscular junctions *in vivo* (36). The Wnt-5a pathway mainly regulates postsynaptic structure and function and, consequently, correlates with the distribution of FZD9. Interestingly, the co-receptor Ror2 also plays a role in the formation of the postsynaptic region and in synaptic development (18), which may suggest a coordinated action between both receptors in Wnt-5a-dependent signaling.

It is known that FZD receptors are able to interact with more than one Wnt ligand, depending on the cellular context. In particular, FZD9 has been shown to bind to Wnt-2 and activates the canonical Wnt pathway, leading to the relocalization of Dvl-1 to the cell membrane in HEK cells (32); however, other studies have indicated that FZD9 interacts with Wnt-7a and activates the Wnt/JNK pathway, mediating the inhibition of lung cancer cells growth (53). Here, we demonstrated that the CRD of FZD9 was able to bind to Wnt-5a and block Wnt-5a-mediated effects in hippocampal neurons, providing direct evidence that FZD9 acts as a functional partner of Wnt-5a. Similarly, we observed that diminished expression of FZD9 by two different short hairpin constructs impaired the Wnt-5a-induced increase in dendritic spine density and eliminated the Wnt-5a-mediated increase in intracellular Ca^{2+} concentrations, indicating that the endogenous expression of FZD9 contributes to Wnt-5a-dependent synaptic formation and signaling activation. Even though we do not discard the possibility that other FZD receptors could be involved in the Wnt-5a pathway in hippocampal neurons, to our knowledge, this is first time that FZD9 has been associated with Wnt-5a signaling in hippocampal neurons. The physiological relevance of these findings relies on the crucial role that this receptor plays in hippocampal development. FZD9 deletion contributes to the neurological symptoms of Williams syndrome, a developmental neurological disorder causing deficits in hippocampal learning (30). Therefore, understanding the function of FZD9 may provide alternatives for the treatment of Williams syndrome.

Our present studies reveal a novel role for Wnt signaling in dendritic spine formation, including a strong interaction between $G\alpha_o$ and FZD9 that is decreased upon Wnt-5a treatment. These findings are consistent with the GPCR nature of FZDs (54). Several studies have demonstrated that G proteins are essential transducers of Wnt signaling (55). Moreover, the $G\alpha_o$ subunit has been related to the Wnt pathway in F9 cells (56) and in *Drosophila melanogaster* (24), but its role in cultured hippocampal neurons had not been clarified. Recently, an interaction between FZD7 and $G\alpha_s$ in C2C12 cells was observed (57). Additionally, a precoupling between FZD6 and $G\alpha_i$ has been demonstrated in HEK cells (58). Interestingly, this precoupling was significantly reduced when the neurons were treated with Wnt-5a, which is similar to our results in hippocampal neurons.

Dendritic spines are plastic structures that experience striking changes in morphology. New dendritic spines develop as long filopodia, which, during the course of spine maturation, exhibit an increase in the spine head width and retract to the dendritic shaft (59). The increase in the spine head width correlates to increased synaptic strength (60). Several factors have been related to the regulation of dendritic spine density, such as BDNF (61), Wnt-7a (10), and Wnt-5a (13). We found that Wnt-5a significantly increased dendritic spine density and increased dendritic spine head width through a $G\alpha_o$ activation-dependent mechanism. In addition, we show that the Wnt-5a induced the activation of PKC, CaMKII, and JNK through the activation of the $G\alpha_o$ subunit. Together, these data suggest that

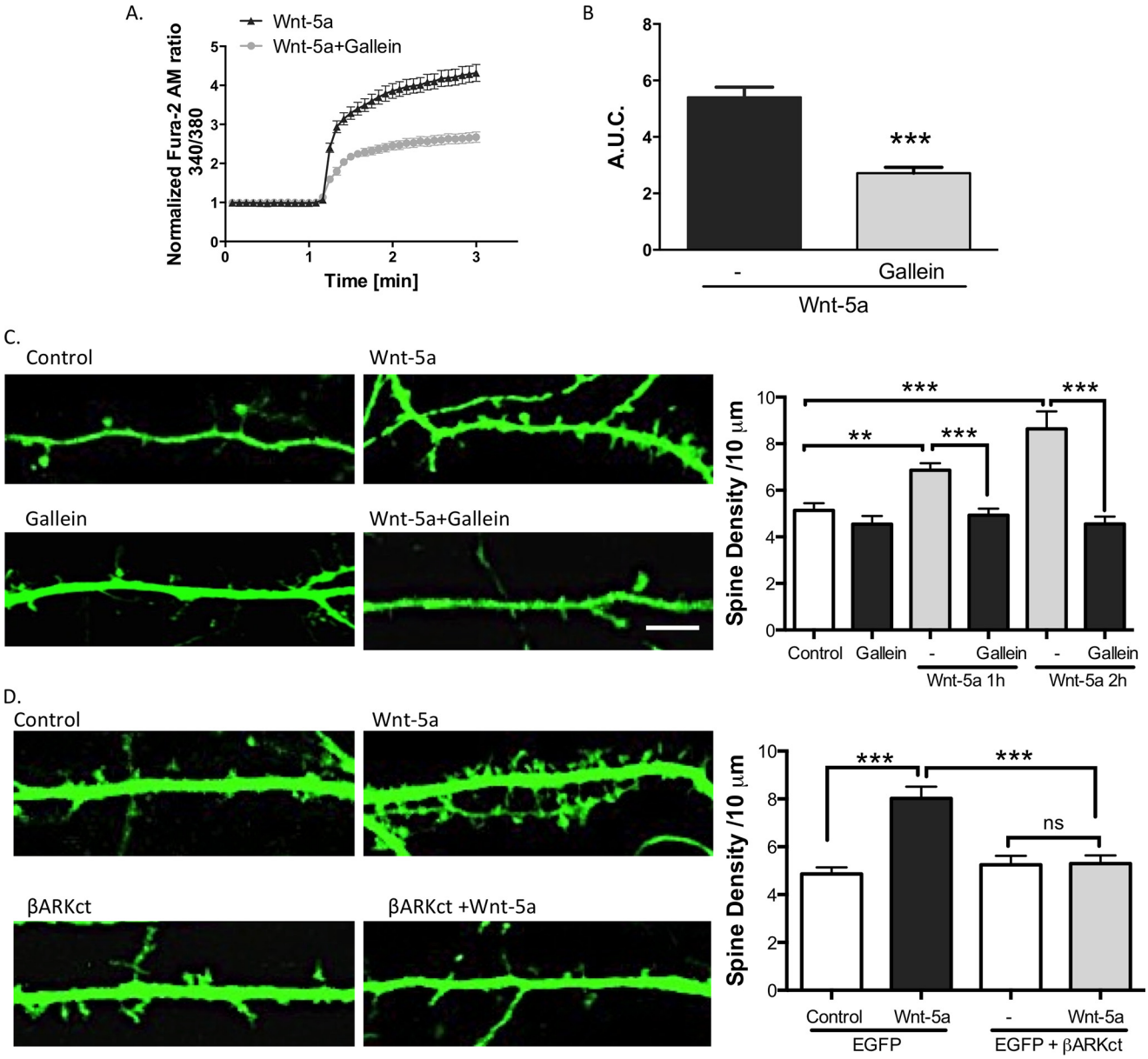

FIGURE 8. **Gallein blocks the Wnt-5a-induced changes in dendritic spine density.** *A*, measurement of the increases in intracellular Ca^{2+} in the hippocampal neurons that were bathed in a Ca^{2+}-free solution and treated with Gallein or Wnt-5a plus Gallein ($n = 3$). *B*, quantification of area under the curve of the measurement of Ca^{2+} concentrations. *C*, images of neurons treated with Wnt-5a and/or Gallein for 2 h. Quantification of the dendritic spine density. *D*, the neurons were transfected with EGFP or EGFP + βARKct and treated with Wnt-5a for 2 h. Quantification of the dendritic spine density ($n = 3$) is shown. *Scale bar*, 3 μm. **, $p < 0.001$; **, $p < 0.01$. *ns*, no significant difference.

the Gα$_o$ subunit is a key factor in the regulation of the formation of dendritic spines and the related signaling cascades.

G proteins are molecular switches that cycle between active GTP-bound and inactive GDP-bound states. Our study suggests that Wnt-5a activates Gα$_o$, without affecting the activation of Gα$_i$, and Gα$_s$, without excluding the involvement of other subunits. Interestingly, Gα$_o$ is highly expressed in the brain (62). The corresponding knock-out mice have neurological impairments, such as reduced motor control, hyperactivity, hyperalgesia, and a shortened lifespan (63). In addition, Gα$_o$ activation is required for the formation of associative memory in mushroom body neurons in *D. melanogaster* (64) and in hippocampal neurons (65).

Interestingly, previous studies indicated a neuroprotective role of Wnt-5a against the effect of Aβ oligomers on synaptic depression, as well as in the reduction of PSD-95 clusters in neuronal cultures (49, 66). Furthermore, the Gα$_o$ subunit has been shown to be involved in Alzheimer's disease, in which the amyloid precursor protein mediates the neuronal toxicity of Aβ oligomers through Gα$_o$ activation (67). It would be interesting to evaluate how these elements interact and how FZD9 is involved in these processes.

Additionally, we provide strong evidence for the involvement of the Gβγ complex in the spinogenic effect of Wnt-5a. We found that in neurons at rest (non-stimulated), Gβγ interacts with Gα$_o$, as reported previously (68) and that this interaction is

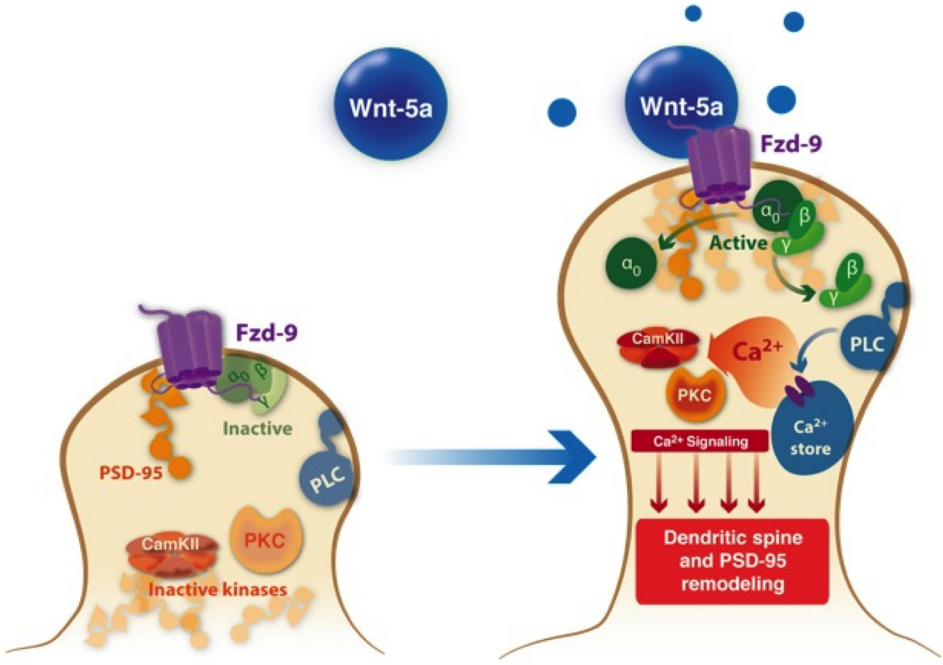

FIGURE 9. **Model for the Wnt-5a effects at the postsynaptic region.** Wnt-5a induces the activation of the non-canonical Wnt pathway by interacting with the FZD9 receptor in the postsynaptic compartment. This interaction facilitates the rapid and transient activation of heterotrimeric G proteins, specifically the $G\alpha_o$ subunit and the $G\beta\gamma$ complex. The activated G proteins participate in the Wnt-5a-induced dendritic spine dynamics and the PSD-95 cluster remodeling through PLC, CaMKII, PKC, and JNK activation.

reduced after Wnt-5a treatment, suggesting that $G\beta\gamma$ is activated and released. The $G\alpha_o$ protein participates in several transduction cascades, although there is good evidence that PLC is a key downstream enzyme in this cascade, and it has also been suggested that $G\beta\gamma$, which activates PLC, mediates this molecular step (69). Additionally, it has been proposed that $G\beta\gamma$ is involved in canonical Wnt signaling through its ability to recruit Dvl to the plasma membrane. Moreover, $G\alpha_o$ directly interacts with Axin to ensure a robust inhibition of the β-catenin destruction complex to allow the activation of canonical Wnt signaling (70). Further experiments will be required to determine the exact molecular mechanisms by which $G\alpha_o$-$G\beta\gamma$ mediates Wnt-5a spinogenesis in hippocampal neurons. In conclusion, we suggest that the cellular mechanism involved in Wnt-5a signaling (Fig. 9) requires the interaction with FZD9 and, consequently, the activation of $G\alpha_o$ and $G\beta\gamma$ to regulate dendritic spine morphogenesis through the non-canonical Wnt pathway.

Experimental Procedures

Reagents—Recombinant Wnt-5a (645-WN/CF), CRD-FZD9 (2440-FZ), CRD-FZD1 (1120-FZ), CRD-FZD2 (1307-FZ), and CRD-FZD5 (1617-FZ) were purchased from R&D Systems. PTX and Gallein were purchased from Sigma-Aldrich. NF449 was from Merck; Fura-2 AM and ionomycin were purchased from Molecular Probes. A/G-agarose beads were purchased from Santa Cruz Biotechnology.

Hippocampal Neuronal Culture—Rat hippocampal cultures were prepared from embryonic day 18 Sprague-Dawley rats of both genders, as previously described (71, 72). On day 2, the cultured neurons were treated with 2 μM cytosine arabinoside for 24 h; this method resulted in cultures that were highly enriched for neurons (~5% glia). The primary hippocampal neurons were cultured in Neurobasal medium supplemented with 1% B27 (Invitrogen) until the experiments were performed. The Bioethical and Biosafety Committee of the Faculty of Biological Sciences of the Pontificia Universidad Católica de Chile approved the experimental procedures.

Receptor Binding Assay—Recombinant CRD-FZD1, CRD-FZD2, CRD-FZD5, or CRD-FZD9 (400 ng/ml) were incubated with 20 μl of A/G-agarose beads and recombinant Wnt-5a (400 ng/ml) for 2 h at 4 °C in 400 μl of lysis buffer from New East Biosciences (catalog no. 30303). Protein A/G-agarose was collected by centrifugation, and the precipitates were washed three times with the lysis buffer. The precipitates from the binding assays were analyzed by SDS-PAGE and probed with goat anti-Wnt-5a AF645 (1:2000) and goat anti-FZD1 (AF1120; 1:1000), goat anti-FZD2 (AF1307; 1:1000), goat anti-FZD5 (AF1617; 1:1000), or goat anti-FZD9 (AF2440; 1:500) antibodies from R&D Systems. For quantifications, the Wnt-5a input band (50 ng) was considered as 100% of signal, and the intensity of the immunoprecipitated bands was compared with the input.

Membrane Fractionation from Rat Brain—Synaptosomes, SYP-enriched fraction (Triton X-100-soluble fraction), and PSD-95-enriched fraction (Triton X-100-insoluble fraction) were isolated as previously described, with some modifications (73). Four rat brains were homogenized for each independent experiment in ice-cold homogenization buffer (4 mM HEPES, pH 7.4, containing 320 mM sucrose and 2 mM EDTA). The homogenate was centrifuged at 710 × *g* for 10 min, and the supernatant was centrifuged at 13,000 × *g* for 20 min. Triton X-100 (1%) was added to the pellet for 2h at 4 °C, which was

then centrifuged at 200,000 × *g* for 2 h. The obtained pellet corresponded to the Triton-X-100-insoluble fraction enriched in PSD-95, and the supernatant contained the Triton-X-100-soluble fraction enriched in SYP. The sample was quantified, and 60 μg of the protein was separated on a 10% SDS-polyacrylamide gel and probed with goat anti-SYP (sc-7568; 1:2000) from Santa Cruz Biotechnology, mouse anti-PSD-95 (k28/43; 1:5000) from Neuromab, and goat anti-FZD9.

Western Blotting—Treated and untreated hippocampal neurons were lysed on ice and either immediately processed or frozen at −150 °C. Immunoblotting was performed as described previously (74). The following primary antibodies were used: goat anti-FZD9, goat anti-FZD5 (AF1617; 1:500), and goat anti-FZD7 (AF198; 1:500) from R&D; mouse anti-CaMKIIα (sc-5306; 1:1000), mouse anti-phospho Tyr^{286}-CAMKIIα (sc-32289; 1:1000), rabbit anti-PKCβII (sc-210; 1:1000), rabbit anti-β-tubulin (sc-9104; 1:1000), mouse anti-β-catenin (sc-7963; 1:1000), and rabbit anti-$G\beta_{1-5}$ (sc-378; 1:1000) from Santa Cruz Biotechnology; rabbit anti-JNK (9252; 1:1000) and rabbit anti-phospho-Thr^{183}/Tyr^{185}-JNK (4668; 1:1000) from Cell Signaling; rabbit phospho-Ser^{660}-PKCβII (ab75837; 1:10000), rabbit anti-$G\alpha_o$ (ab136535; 1:5000), and rabbit anti-$G\alpha_i$ (ab20392; 1:1000) from Abcam; mouse anti-PSD95 (k28/43; 1:10000) from University of California at Davis/National Institutes of Health NeuroMab Facility; and mouse anti-β-actin (A5316; 1:10000) from Sigma. Equal amounts of protein were loaded (20 μg).

Immunofluorescence, Transfection, and Image Analysis—The hippocampal neurons were cultured on coverslips at a density of 35,000 cells/coverslip, subjected to different treatments, and fixed with a freshly prepared 4% paraformaldehyde plus 4% sucrose in PBS for 20 min at 4 °C. The cells were then permeabilized with 0.2% Triton X-100 for 5 min at room temperature and then blocked with 1% bovine serum albumin in PBS (blocking solution) for 30 min at 37 °C, followed by an overnight incubation with the mouse anti-PSD-95 k28/43 (1:400), rabbit anti-Piccolo 142002 (1:300) from Synaptic Systems and/or goat anti-FZD9 (1:100) primary antibodies at 4 °C. The cells were thoroughly washed with PBS and then incubated with phalloidin coupled to Alexa Fluor 633 (1:500) from Molecular Probes, which was used as a neurite marker, and with secondary antibodies coupled to Alexa Fluor 488 and Alexa Fluor 546 (1:1000) from Molecular Probes for 30 min at 37 °C. The coverslips were mounted in Fluoromount G mounting medium. Digital images were captured with an Olympus FV 1000 confocal microscope. The images were analyzed using National Institutes of Health ImageJ software. The images of the PSD-95 staining were captured from 10 microscope fields for each condition in three or four independent experiments. Each field contained processes for one or two neurons, in which two or three phalloidin-labeled neurites/neurons were selected and analyzed. We used a previously described protocol to quantify the PSD-95 clusters (11).

To transfect the cultured neurons, we performed magnetofection using NeuroMag (OZ Bioscience) using neurons at DIV 10 and 11 that were plated at 60,000–100,000 cells/35-mm poly-D-lysine-coated glass-bottomed dish. The following constructs were used: EGFP (Clontech); Fux (control plasmid); shFZD9-EGFP (36); commercial scramble-FZD9 and shFZD9-EGFP#3 from Qiagen (catalog no. KH02416G); $G\alpha_o$PTXi; $G\alpha_{i2}$PTXi; $G\alpha_{i3}$PTXi; and βARKct provided by Dr. J. Silvio Gutkind (National Institute of Health, Bethesda). First, the neurons were washed for 30 min with Neurobasal medium. Then 0.8 μg of DNA/1.25 μl of magneto beads were mixed and incubated at *D. melanogaster* for 15 min in 100 μl of Neurobasal medium. In the co-transfection experiments, the mix was prepared using 0.4 μg of EGFP plus 0.4 μg of $G\alpha_o$PTXi, $G\alpha_{i2/3}$PTXi or βARKct plus 1.25 μl of the beads. Next, the mix was added to the neurons for 15 min with the magnet in the bottom of the plate; it was removed 40 min later, and the transfection medium was replaced with fresh medium. At 14 DIV, the hippocampal neurons were starved for 2 h with Neurobasal medium without the B27 supplement before the treatments with recombinant Wnt-5a (300 ng/ml = 7,3 nM) with or without PTX (150 ng/ml), Gallein (5 μM), NF449 (5 μM), or CRD-FZD9 (300 ng/ml) for different time periods. An Olympus Fluo View FV 1000 confocal microscope was used to obtain the digital images at a resolution of 1024 × 1024. To quantify the dendritic spines and for three-dimensional imaging, the *Z* stack images were reconstructed using the super-pass module of the Imaris software. The dendritic shafts and spines were manually traced using the filament mode. The protrusions below the 3 μm were considered for the three-dimensional reconstruction. Accurate reconstructions of the diameter of the spine neck and head were created using the diameter function with a contrast threshold of 0.8. Ten microscopic fields were imaged for each condition in three to five independent experiments. To determine the spine length and the spine head width, the mean of all spines from each neurite was measured. The spine density was calculated by measuring the total number of spines/dendrite length (spine density/10 μm) for each condition.

Measurements of Intracellular Ca^{2+} Mobilization in Hippocampal Rat Neurons—Ca^{2+} variations were determined in cells loaded with 4.5 μM Fura-2 AM at 37 °C for 30 min (75) using DIV 10 hippocampal neurons transfected with Fux-EGFP or shFZD9-EGFP at DIV 7 or non-transfected neurons. The experiments were performed with two different isotonic solutions: one containing calcium, 1.2 mM $CaCl_2$, 140 mM NaCl, 5 mM KCl, 0.5 mM $MgCl_2$, 5 mM glucose, and 10 mM HEPES (305 mOsm/liter, pH 7.4, with Tris); and one without calcium, 0 mM $CaCl_2$, 140 mM NaCl, 2.5 mM KCl, 1.7 mM $MgCl_2$, 5 mM glucose, 0.5 mM EGTA, and 10 mM HEPES (305 mOsm/liter, pH 7.4, with Tris). Cytosolic Ca^{2+} levels were continuously recorded in the isotonic solution for 1 min before (basal Ca^{2+} level) and 3 min after Wnt-5a application. After 4 min, 1 μM ionomycin was added as a positive control for Ca^{2+} increase. The increases in cytosolic Ca^{2+} were represented as the normalized ratio of the emitted fluorescence at 510 nm after excitation at 340 and 380 nm relative to the ratio measured prior to stimulation (first minute before application of the stimuli), and the A.U.C. after the addition of Wnt-5a was integrated. This integration was performed using the GraphPad Software Prism 6. We used the Olympus spinning disc IX81 microscope to perform the live Ca^{2+} imaging experiments.

HT22 Cell Transfections—Immortalized HT22 cells from mouse hippocampal neuronal cells were co-transfected with

0.5 μg of shFZD9-EGFP or Fux-EGFP plasmids using Lipofectamine™ 2000 (Invitrogen) 48 h after plating in 6-well culture plates at a density of 1.6×10^6 cells/well.

Immunoprecipitation of $G\alpha_{i/o}$ Proteins—We used the $G\alpha_o$ (80901) and $G\alpha_i$ (80301) activation assay kits from New East Biosciences. The cultured hippocampal neurons were seeded at a density of 900,000 cells/well at DIV 14 and were treated with Wnt-5a (300 ng/ml). After treatment, cells were lysed, and the amount of protein was quantified. The same amount of protein was used in each condition for the immunoprecipitation (400 μg) with the specific antibodies that recognize the GTP-bound $G\alpha_o$ or the GTP-bound $G\alpha_i$ proteins according to the manufacturer's recommended protocol. GTPγS was used as a positive control and was added to the neuronal lysate and incubated for 90 min at room temperature before immunoprecipitation. The total level of protein was detected by immunoblot with the mouse anti-$G\alpha_o$ (1:1000) or mouse anti-$G\alpha_i$ (1:1000) antibodies from the activation kits from New East Bioscience.

For immunoprecipitation of total $G\alpha_o$ hippocampal cultured neurons were seeded at a density of 600,000 cells/well. The neurons were treated with vehicle or Wnt-5a and then lysed. After protein quantification, 400 μg of protein was incubated with 5 μg/ml of mouse anti-$G\alpha_o$ (sc-13532; Santa Cruz Biotechnology) and 20 μl of agarose beads for 1 h at 4 °C with orbital rotation. The 10% of the sample was used as input. Next, the lysates were washed three times and suspended in 20 μl of Laemmli 2× loading buffer. The samples were analyzed by immunoblotting with rabbit anti-$G\alpha_o$, goat anti-FZD9, and rabbit anti-$G\beta_{1-5}$ antibodies.

Statistical Analyses—Statistical analysis was performed using the statistical software Prism 5 (GraphPad Software). The values are expressed as the means ± S.E. of the means. The statistical significance of the differences was assessed using one-way analysis of variance with Bonferroni's post test for multiple comparisons and Student's *t* test for comparisons between two conditions ($p < 0.05$ was considered significant). The number of independent experiments is indicated in the corresponding figure legend.

Author Contributions—V. T. R. and N. C. I. designed and coordinated the study and wrote the manuscript. V. T. R. performed and analyzed the immunofluorescence and Western blotting experiments. E. R.-F. performed and analyzed the experiments shown in Figs. 1*D*, 2 (*B* and *C*), 4 (*C* and *D*), and 8 (*A* and *B*). J. P. H. and A. L. provided technical assistance and contributed to the preparation of the figures and the manuscript. All authors reviewed the results and approved the final version of the manuscript.

References

1. Oliva, C. A., Vargas, J. Y., and Inestrosa, N. C. (2013) Wnts in adult brain: from synaptic plasticity to cognitive deficiencies. *Front. Cell Neurosci.* **7,** 224
2. Willert, K., and Nusse, R. (2012) Wnt proteins. *Cold Spring Harb. Perspect. Biol.* **4,** a007864
3. Budnik, V., and Salinas, P. C. (2011) Wnt signaling during synaptic development and plasticity. *Curr. Opin. Neurobiol.* **21,** 151–159
4. Inestrosa, N. C., and Arenas, E. (2010) Emerging roles of Wnts in the adult nervous system. *Nat. Rev. Neurosci.* **11,** 77–86
5. Park, M., and Shen, K. (2012) WNTs in synapse formation and neuronal circuitry. *EMBO J.* **31,** 2697–2704
6. Purro, S. A., Galli, S., and Salinas, P. C. (2014) Dysfunction of Wnt signaling and synaptic disassembly in neurodegenerative diseases. *J. Mol. Cell Biol.* **6,** 75–80
7. Vargas, J. Y., Fuenzalida, M., and Inestrosa, N. C. (2014) *In vivo* activation of Wnt signaling pathway enhances cognitive function of adult mice and reverses cognitive deficits in an Alzheimer's disease model. *J. Neurosci.* **34,** 2191–2202
8. Cerpa, W., Godoy, J. A., Alfaro, I., Farías, G. G., Metcalfe, M. J., Fuentealba, R., Bonansco, C., and Inestrosa, N. C. (2008) Wnt-7a modulates the synaptic vesicle cycle and synaptic transmission in hippocampal neurons. *J. Biol. Chem.* **283,** 5918–5927
9. Ahmad-Annuar, A., Ciani, L., Simeonidis, I., Herreros, J., Fredj, N. B., Rosso, S. B., Hall, A., Brickley, S., and Salinas, P. C. (2006) Signaling across the synapse: a role for Wnt and Dishevelled in presynaptic assembly and neurotransmitter release. *J. Cell Biol.* **174,** 127–139
10. Ciani, L., Boyle, K. A., Dickins, E., Sahores, M., Anane, D., Lopes, D. M., Gibb, A. J., and Salinas, P. C. (2011) Wnt7a signaling promotes dendritic spine growth and synaptic strength through Ca^{2+}/Calmodulin-dependent protein kinase II. *Proc. Natl. Acad. Sci. U.S.A.* **108,** 10732–10737
11. Farías, G. G., Alfaro, I. E., Cerpa, W., Grabowski, C. P., Godoy, J. A., Bonansco, C., and Inestrosa, N. C. (2009) Wnt-5a/JNK signaling promotes the clustering of PSD-95 in hippocampal neurons. *J. Biol. Chem.* **284,** 15857–15866
12. Muñoz, F. J., Godoy, J. A., Cerpa, W., Poblete, I. M., Huidobro-Toro, J. P., and Inestrosa, N. C. (2014) Wnt-5a increases NO and modulates NMDA receptor in rat hippocampal neurons. *Biochem. Biophys. Res. Commun.* **444,** 189–194
13. Varela-Nallar, L., Alfaro, I. E., Serrano, F. G., Parodi, J., and Inestrosa, N. C. (2010) Wingless-type family member 5A (Wnt-5a) stimulates synaptic differentiation and function of glutamatergic synapses. *Proc. Natl. Acad. Sci. U.S.A.* **107,** 21164–21169
14. Niehrs, C. (2012) The complex world of WNT receptor signalling. *Nat. Rev. Mol. Cell Biol.* **13,** 767–779
15. Sato, A., Yamamoto, H., Sakane, H., Koyama, H., and Kikuchi, A. (2010) Wnt5a regulates distinct signalling pathways by binding to Frizzled2. *EMBO J.* **29,** 41–54
16. Nishita, M., Itsukushima, S., Nomachi, A., Endo, M., Wang, Z., Inaba, D., Qiao, S., Takada, S., Kikuchi, A., and Minami, Y. (2010) Ror2/Frizzled complex mediates Wnt5a-induced AP-1 activation by regulating Dishevelled polymerization. *Mol. Cell. Biol.* **30,** 3610–3619
17. Onishi, K., Shafer, B., Lo, C., Tissir, F., Goffinet, A. M., and Zou, Y. (2013) Antagonistic functions of Dishevelleds regulate Frizzled3 endocytosis via filopodia tips in Wnt-mediated growth cone guidance. *J. Neurosci.* **33,** 19071–19085
18. Alfaro, I. E., Varela-Nallar, L., Varas-Godoy, M., and Inestrosa, N. C. (2015) The ROR2 tyrosine kinase receptor regulates dendritic spine morphogenesis in hippocampal neurons. *Mol. Cell. Neurosci.* **67,** 22–30
19. Gordon, M. D., and Nusse, R. (2006) Wnt signaling: multiple pathways, multiple receptors, and multiple transcription factors. *J. Biol. Chem.* **281,** 22429–22433
20. Kilander, M. B., Halleskog, C., and Schulte, G. (2011) Recombinant WNTs differentially activate β-catenin-dependent and -independent signalling in mouse microglia-like cells. *Acta Physiol.* **203,** 363–372
21. Koval, A., and Katanaev, V. L. (2011) Wnt3a stimulation elicits G-protein-coupled receptor properties of mammalian Frizzled proteins. *Biochem. J.* **433,** 435–440
22. Milligan, G., and Kostenis, E. (2006) Heterotrimeric G-proteins: a short history. *Br. J. Pharmacol.* **147,** S46–S55
23. Neer, E. J. (1995) Heterotrimeric G proteins: organizers of transmembrane signals. *Cell* **80,** 249–257
24. Katanaev, V. L., Ponzielli, R., Sémériva, M., and Tomlinson, A. (2005) Trimeric G protein-dependent frizzled signaling in *Drosophila*. *Cell* **120,** 111–122
25. Dejmek, J., Säfholm, A., Kamp Nielsen, C., Andersson, T., and Leandersson, K. (2006) Wnt-5a/Ca2+-induced NFAT activity is counteracted by Wnt-5a/Yes-Cdc42-casein kinase 1α signaling in human mammary epithelial cells. *Mol. Cell. Biol.* **26,** 6024–6036
26. Ma, L., and Wang, H. Y. (2006) Suppression of cyclic GMP-dependent

protein kinase is essential to the Wnt/cGMP/Ca2+ pathway. *J. Biol. Chem.* **281,** 30990–31001
27. Halleskog, C., Dijksterhuis, J. P., Kilander, M. B., Becerril-Ortega, J., Villaescusa, J. C., Lindgren, E., Arenas, E., and Schulte, G. (2012) Heterotrimeric G protein-dependent WNT-5A signaling to ERK1/2 mediates distinct aspects of microglia proinflammatory transformation. *J. Neuroinflammation* **9,** 111
28. Li, Y., Tian, C., Yang, Y., Yan, Y., Ni, Y., Wei, Y., Pleasure, S. J., and Zhao, C. (2011) An inducible transgenic Cre mouse line for the study of hippocampal development and adult neurogenesis. *Genesis* **49,** 919–926
29. Shah, S. M., Kang, Y. J., Christensen, B. L., Feng, A. S., and Kollmar, R. (2009) Expression of Wnt receptors in adult spiral ganglion neurons: frizzled 9 localization at growth cones of regenerating neurites. *Neuroscience* **164,** 478–487
30. Zhao, C., Avilés, C., Abel, R. A., Almli, C. R., McQuillen, P., and Pleasure, S. J. (2005) Hippocampal and visuospatial learning defects in mice with a deletion of frizzled 9, a gene in the Williams syndrome deletion interval. *Development* **132,** 2917–2927
31. Varela-Nallar, L., Ramirez, V. T., Gonzalez-Billault, C., and Inestrosa, N. C. (2012) Frizzled receptors in neurons: from growth cones to the synapse. *Cytoskeleton* **69,** 528–534
32. Karasawa, T., Yokokura, H., Kitajewski, J., and Lombroso, P. J. (2002) Frizzled-9 is activated by Wnt-2 and functions in Wnt/β-catenin signaling. *J. Biol. Chem.* **277,** 37479–37486
33. Momoi, A., Yoda, H., Steinbeisser, H., Fagotto, F., Kondoh, H., Kudo, A., Driever, W., and Furutani-Seiki, M. (2003) Analysis of Wnt8 for neural posteriorizing factor by identifying Frizzled 8c and Frizzled 9 as functional receptors for Wnt8. *Mech. Dev.* **120,** 477–489
34. Winn, R. A., Van Scoyk, M., Hammond, M., Rodriguez, K., Crossno, J. T., Jr., Heasley, L. E., and Nemenoff, R. A. (2006) Antitumorigenic effect of Wnt 7a and Fzd 9 in non-small cell lung cancer cells is mediated through ERK-5-dependent activation of peroxisome proliferator-activated receptor γ. *J. Biol. Chem.* **281,** 26943–26950
35. Dann, C. E., Hsieh, J. C., Rattner, A., Sharma, D., Nathans, J., and Leahy, D. J. (2001) Insights into Wnt binding and signalling from the structures of two Frizzled cysteine-rich domains. *Nature* **412,** 86–90
36. Avilés, E. C., Pinto, C., Hanna, P., Ojeda, J., Pérez, V., De Ferrari, G. V., Zamorano, P., Albistur, M., Sandoval, D., and Henríquez, J. P. (2014) Frizzled-9 impairs acetylcholine receptor clustering in skeletal muscle cells. *Front. Cell. Neurosci.* **8,** 110
37. Kohn, A. D., and Moon, R. T. (2005) Wnt and calcium signaling: β-catenin-independent pathways. *Cell Calcium* **38,** 439–446
38. Cuitino, L., Godoy, J. A., Farías, G. G., Couve, A., Bonansco, C., Fuenzalida, M., and Inestrosa, N. C. (2010) Wnt-5a modulates recycling of functional GABAA receptors on hippocampal neurons. *J. Neurosci.* **30,** 8411–8420
39. Stein, P. E., Boodhoo, A., Armstrong, G. D., Cockle, S. A., Klein, M. H., and Read, R. J. (1994) The crystal structure of pertussis toxin. *Structure* **2,** 45–57
40. Plaut, R. D., and Carbonetti, N. H. (2008) Retrograde transport of pertussis toxin in the mammalian cell. *Cell. Microbiol.* **10,** 1130–1139
41. Hohenegger, M., Waldhoer, M., Beindl, W., Böing, B., Kreimeyer, A., Nickel, P., Nanoff, C., and Freissmuth, M. (1998) Gsα-selective G protein antagonists. *Proc. Natl. Acad. Sci. U.S.A.* **95,** 346–351
42. Cabrera-Vera, T. M., Vanhauwe, J., Thomas, T. O., Medkova, M., Preininger, A., Mazzoni, M. R., and Hamm, H. E. (2003) Insights into G protein structure, function, and regulation. *Endocr. Rev.* **24,** 765–781
43. Halleskog, C., and Schulte, G. (2013) Pertussis toxin-sensitive heterotrimeric G($\alpha_{i/o}$) proteins mediate WNT/β-catenin and WNT/ERK1/2 signaling in mouse primary microglia stimulated with purified WNT-3A. *Cell. Signal.* **25,** 822–828
44. Bonacci, T. M., Mathews, J. L., Yuan, C., Lehmann, D. M., Malik, S., Wu, D., Font, J. L., Bidlack, J. M., and Smrcka, A. V. (2006) Differential targeting of Gβγ-subunit signaling with small molecules. *Science* **312,** 443–446
45. Belkouch, M., Dansereau, M. A., Réaux-Le Goazigo, A., Van Steenwinckel, J., Beaudet, N., Chraibi, A., Melik-Parsadaniantz, S., and Sarret, P. (2011) The chemokine CCL2 increases Nav1.8 sodium channel activity in primary sensory neurons through a Gβγ-dependent mechanism. *J. Neurosci.* **31,** 18381–18390
46. Pitcher, J. A., Touhara, K., Payne, E. S., and Lefkowitz, R. J. (1995) Pleckstrin homology domain-mediated membrane association and activation of the β-adrenergic receptor kinase requires coordinate interaction with Gβγ subunits and lipid. *J. Biol. Chem.* **270,** 11707–11710
47. Oliva, C. A., Vargas, J. Y., and Inestrosa, N. C. (2013) Wnt signaling: role in LTP, neural networks and memory. *Ageing Res. Rev.* **12,** 786–800
48. Beaumont, V., Thompson, S. A., Choudhry, F., Nuthall, H., Glantschnig, H., Lipfert, L., David, G. R., Swain, C. J., McAllister, G., and Munoz-Sanjuan, I. (2007) Evidence for an enhancement of excitatory transmission in adult CNS by Wnt signaling pathway modulation. *Mol. Cell Neurosci.* **35,** 513–524
49. Cerpa, W., Farías, G. G., Godoy, J. A., Fuenzalida, M., Bonansco, C., and Inestrosa, N. C. (2010) Wnt-5a occludes Aβ oligomer-induced depression of glutamatergic transmission in hippocampal neurons. *Mol. Neurodegener.* **5,** 3
50. Cerpa, W., Latorre-Esteves, E., and Barria, A. (2015) RoR2 functions as a noncanonical Wnt receptor that regulates NMDAR-mediated synaptic transmission. *Proc. Natl. Acad. Sci. U.S.A.* **112,** 4797–4802
51. Cerpa, W., Gambrill, A., Inestrosa, N. C., and Barria, A. (2011) Regulation of NMDA-receptor synaptic transmission by Wnt signaling. *J. Neurosci.* **31,** 9466–9471
52. Zhao, C., and Pleasure, S. J. (2004) Frizzled-9 promoter drives expression of transgenes in the medial wall of the cortex and its chief derivative the hippocampus. *Genesis* **40,** 32–39
53. Winn, R. A., Marek, L., Han, S. Y., Rodriguez, K., Rodriguez, N., Hammond, M., Van Scoyk, M., Acosta, H., Mirus, J., Barry, N., Bren-Mattison, Y., Van Raay, T. J., Nemenoff, R. A., and Heasley, L. E. (2005) Restoration of Wnt-7a expression reverses non-small cell lung cancer cellular transformation through frizzled-9-mediated growth inhibition and promotion of cell differentiation. *J. Biol. Chem.* **280,** 19625–19634
54. Dijksterhuis, J. P., Petersen, J., and Schulte, G. (2014) WNT/Frizzled signalling: receptor-ligand selectivity with focus on FZD-G protein signalling and its physiological relevance: IUPHAR Review 3. *Br. J. Pharmacol.* **171,** 1195–1209
55. Malbon, C. C. (2005) β-Catenin, cancer, and G proteins: not just for frizzleds anymore. *Sci. STKE* **2005,** pe35
56. Feigin, M. E., and Malbon, C. C. (2007) RGS19 regulates Wnt-β-catenin signaling through inactivation of Gα$_o$. *J. Cell Sci.* **120,** 3404–3414
57. von Maltzahn, J., Bentzinger, C. F., and Rudnicki, M. A. (2012) Wnt7a-Fzd7 signalling directly activates the Akt/mTOR anabolic growth pathway in skeletal muscle. *Nat. Cell Biol.* **14,** 186–191
58. Kilander, M. B., Petersen, J., Andressen, K. W., Ganji, R. S., Levy, F. O., Schuster, J., Dahl, N., Bryja, V., and Schulte, G. (2014) Disheveled regulates precoupling of heterotrimeric G proteins to Frizzled 6. *FASEB J.* **28,** 2293–2305
59. Zito, K., Scheuss, V., Knott, G., Hill, T., and Svoboda, K. (2009) Rapid functional maturation of nascent dendritic spines. *Neuron* **61,** 247–258
60. Yang, Y., Wang, X. B., Frerking, M., and Zhou, Q. (2008) Spine expansion and stabilization associated with long-term potentiation. *J. Neurosci.* **28,** 5740–5751
61. Hiester, B. G., Galati, D. F., Salinas, P. C., and Jones, K. R. (2013) Neurotrophin and Wnt signaling cooperatively regulate dendritic spine formation. *Mol. Cell. Neurosci.* **56,** 115–127
62. Nüsse, O., and Neer, E. J. (1996) Localization of Gα$_o$ to growth cones in PC12 cells: role of Gα$_o$ association with receptors and Gβγ. *J. Cell Sci.* **109,** 221–228
63. Jiang, M., Gold, M. S., Boulay, G., Spicher, K., Peyton, M., Brabet, P., Srinivasan, Y., Rudolph, U., Ellison, G., and Birnbaumer, L. (1998) Multiple neurological abnormalities in mice deficient in the G protein G$_o$. *Proc. Natl. Acad. Sci. U.S.A.* **95,** 3269–3274
64. Ferris, J., Ge, H., Liu, L., and Roman, G. (2006) G$_o$ signaling is required for *Drosophila* associative learning. *Nat. Neurosci.* **9,** 1036–1040
65. Ramírez, V. T., Ramos-Fernández, E., and Inestrosa, N. C. (2016) The Gα$_o$ activator mastoparan-7 promotes dendritic spine formation in hippocampal neurons. *Neural Plast.* **2016,** 4258171
66. Silva-Alvarez, C., Arrázola, M. S., Godoy, J. A., Ordenes, D., and Inestrosa, N. C. (2013) Canonical Wnt signaling protects hippocampal neurons from Aβ oligomers: role of non-canonical Wnt-5a/Ca^{2+} in mitochondrial dynamics. *Front. Cell. Neurosci.* **7,** 97

67. Sola Vigo, F., Kedikian, G., Heredia, L., Heredia, F., Añel, A. D., Rosa, A. L., and Lorenzo, A. (2009) Amyloid-β precursor protein mediates neuronal toxicity of amyloid β through G_o protein activation. *Neurobiol. Aging* **30,** 1379–1392
68. Exner, T., Jensen, O. N., Mann, M., Kleuss, C., and Nürnberg, B. (1999) Posttranslational modification of $G\alpha_{o1}$ generates $G\alpha_{o3}$, an abundant G protein in brain. *Proc. Natl. Acad. Sci. U.S.A.* **96,** 1327–1332
69. Rünnenburger, K., Breer, H., and Boekhoff, I. (2002) Selective G protein $\beta\gamma$-subunit compositions mediate phospholipase C activation in the vomeronasal organ. *Eur J. Cell Biol.* **81,** 539–547
70. Egger-Adam, D., and Katanaev, V. L. (2010) The trimeric G protein G_o inflicts a double impact on axin in the Wnt/Frizzled signaling pathway. *Dev. Dyn.* **239,** 168–183
71. Alvarez, A. R., Godoy, J. A., Mullendorff, K., Olivares, G. H., Bronfman, M., and Inestrosa, N. C. (2004) Wnt-3a overcomes β-amyloid toxicity in rat hippocampal neurons. *Exp. Cell Res.* **297,** 186–196
72. Caceres, A., Binder, L. I., Payne, M. R., Bender, P., Rebhun, L., and Steward, O. (1984) Differential subcellular localization of tubulin and the microtubule-associated protein MAP2 in brain tissue as revealed by immunocytochemistry with monoclonal hybridoma antibodies. *J. Neurosci.* **4,** 394–410
73. Spalloni, A., Origlia, N., Sgobio, C., Trabalza, A., Nutini, M., Berretta, N., Bernardi, G., Domenici, L., Ammassari-Teule, M., and Longone, P. (2011) Postsynaptic alteration of NR2A subunit and defective autophosphorylation of αCaMKII at threonine-286 contribute to abnormal plasticity and morphology of upper motor neurons in presymptomatic SOD1G93A mice, a murine model for amyotrophic lateral sclerosis. *Cerebral Cortex* **21,** 796–805
74. Varela-Nallar, L., Grabowski, C. P., Alfaro, I. E., Alvarez, A. R., and Inestrosa, N. C. (2009) Role of the Wnt receptor Frizzled-1 in presynaptic differentiation and function. *Neural Dev.* **4,** 41
75. Fernandes, J., Lorenzo, I. M., Andrade, Y. N., Garcia-Elias, A., Serra, S. A., Fernández-Fernández, J. M., and Valverde, M. A. (2008) IP3 sensitizes TRPV4 channel to the mechano- and osmotransducing messenger 5′-6′-epoxyeicosatrienoic acid. *J. Cell Biol.* **181,** 143–155